Gutiérrez-Urzúa, L.F., Freddi, F., Di Sarno, L. (2020). Critical Comparison of Assessment Codes for Steel Moment Resisting Frames. The 9th European Conference on Steel and Composite Structures (Eurosteel 2020), Sheffield, UK, 1–3 September 2021. https://doi.org/10.1002/cepa.1390

Critical Comparison of Assessment Codes for Steel Moment Resisting Frames

Fernando Gutiérrez-Urzúa, Fabio Freddi[1], Luigi Di Sarno[2]

Correspondence

Fernando Gutiérrez-Urzúa
University College London
Civil, Environmental and Geomatic Engineering
Chadwick Building, Gower St.
WC1E 6BT London, UK
Email: f.urzua@ucl.ac.uk

Abstract

Many existing steel multi-storey frame buildings worldwide were designed prior to the introduction of modern seismic design provisions or based on outdated hazard maps considering low values of seismic intensity. This often resulted in buildings showing low performances with respect to earthquake loads. Assessment codes, such as the Eurocode 8 Part 3 and the ASCE 41, have been conceived to provide tools to assess the seismic performance of existing structures, to evaluate their adequacy with respect to the current safety standards and the need for seismic retrofit. However, recent research studies have revealed the necessity for a revision of these codes. In particular, for steel moment resisting frames, the current European regulation shares many similarities with older versions of the American codes, but has failed to incorporate changes based on the state-of-the-art knowledge. In addition, the undergoing update of other parts of the Eurocode motivates a full revision of the current standards. This paper compares the assessment procedures of the European and American codes. Two low-code steel Moment Resisting Frames were considered for case study purposes and the assessment was performed based on three local Engineering Demand Parameters (EDPs), *i.e.*, column's rotation, beam's rotation and panel zone's shear distortion, and the inter-story drift as global EDP. Incremental Dynamic Analyses were performed for the development of component and system fragility curves. The present work aims to identify some challenges and to provide some preliminary insights for the revision of the Eurocode 8 Part 3.

Keywords

Existing steel frames, Seismic response, Seismic Assessment, Local engineering demand parameters, Fragility curves, Eurocode 8 Part 3, ASCE 41

1 Introduction

The development of bolted and welded rigid and semi-rigid connections increased the efficiency and popularity of steel Moment Resisting Frames (MRFs) in countries such as US, Mexico, Japan, China and Iran (*e.g.*, [1, 2]). Although these structures showed an apparently satisfactory performance after strong earthquakes (*e.g.*, 1985 Mexico City, 1971 San Fernando, 1964 Prince William Sound), further inspections revealed several deficiencies, which confronted the common practices and regulations dictated by the codes. As a result, new material developments (such as the ASTM A992) and new design philosophies (such as the capacity design) were introduced in seismic design regulations [1].

However, many existing structures have been built before the introduction of these modern seismic design codes and are often characterised by deficiencies typical of old design practices. These include lack of strength and stiffness hierarchy rules (*i.e.*, no capacity design), use of flexible panel zones, low-ductility (*i.e.*, no energy dissipation), etc. Hence, there is a significant need for advanced assessment procedures to evaluate the seismic performances of these structures, their adequacy with respect to the current safety standards and the need for seismic retrofit.

The assessment of existing structures within European countries is performed according to the Eurocode 8 Part 3 [3] (EC8-3). This code defines three qualitative limit states in a performance-based framework, corresponding to different levels of the expected damage. Each limit state is related from one side to the probability of occurrence of earthquakes with a defined seismic intensity and, from the other side to the capacity limits of specific components. However, for some components, these capacity limits fail to consider simultaneous effects which may lead to the overestimation of the capacity, as previously pointed out by Araújo and Castro [4]. In addition, some of these established limits do not have a clear background and seem to be simply adapted from similar American regulations [5].

On the other hand, the newest version of the ASCE 41 [6] (ASCE41-

1. University College London, London, UK.
2. University of Liverpool, Liverpool, UK.

17) is the result of almost two decades of evolution of its predecessors (*i.e.*, ASCE 41-13 [7], ASCE 41-06 [8]) and incorporates parameters to account for simultaneous effect of actions and provides demand-dependent capacity limits defined based on experimental data. However, in some cases, the complexity of its approach may limit its use in practical applications.

Araújo *et al.* [9] investigated the current capacity limits in the European code by creating and analysing detailed finite element models, considering the influence of member imperfections, axial load and using real ground motion records. The outcomes of this work highlighted that "the EC8-3 limits systematically overestimate the deformation capacity of deep and slender web cross-section profiles" and that it "is even more pronounced for cases in which the member is subjected to axial load". Successively, Araújo and Castro [5] compared the EC8-3 and the ASCE 41-13 [7] for steel buildings and compared the structural response of two case study buildings subjected to these regulations. The outcomes of this study allowed to highlight some of the limitations of the EC8-3 capacity limits and, amongst others, they found that these limits may be inadequate considering that they were adapted from the American codes, and therefore, were calibrated based on the performance of American steel profiles. The outcomes of these studies highlight the need for significant efforts of the research community toward the definition of more adequate provisions for the assessment of existing steel structures that can accurately describe the performance of deficient structures, especially within European countries.

Another aspect that need careful consideration regards the influence of the uncertainties involved in the problem. In fact, the seismic response of the structure is affected by uncertainties in the earthquake input (*i.e.*, record-to-record variability), in the properties defining the system (*i.e.*, model parameter uncertainty), and by lack of knowledge (*i.e.*, epistemic uncertainty). The EC8-3 [3] considers the epistemic uncertainty by including confidence factors (CF_{KLn}) that directly reduce the capacity of the structural elements, depending on the knowledge level of the structure (*i.e.*, material testing, drawings availability, surveying process). In a similar way, the ASCE41-17 [6] provides a knowledge factor (κ). Previous studies demonstrated that the effects of model parameter uncertainty and epistemic uncertainty are usually less notable than the effects of record-to-record variability [10, 11], and they are not considered in this study. In addition, full knowledge of the structures is assumed in the present paper. A popular approach to consider the influence of the record-to-record variability in the seismic vulnerability assessment of structural systems involves the development of fragility curves (*e.g.*, [5, 12, 13]). These tools provide the probability of exceeding a specified damage state or a defined failure condition for different levels of seismic intensity, measured by using an appropriate Intensity Measure (IM) (*e.g.*, [14]).

Several studies investigated the seismic performances of existing structures by accounting for the uncertainties related to the seismic input. For example, Molina Hutt *et al.* [15] investigated the vulnerability of steel MRF built in the 1970s by using the conditional spectrum method [16] based in 20 ground motions recorded in west USA. Similarly, Zareian and Krawinkler [17] studied the collapse potential of an 8-storey MRF to illustrate the effects of the uncertainties in the conceptual design for collapse safety. However, these studies considered only global EDPs such as the peak inter-story drifts (IDR), which may be inadequate when assessing the seismic performance of a low-code existing structure. In fact, in existing frames, due to the lack of modern design seismic rules such as strength hierarchy (*i.e.*, capacity design), there may be no relationship between local failures and global EDPs. This means that IDR may not be able to reflect the deficiencies of the structural elements at a local level [13]. Therefore, while accounting also for the uncertainties related to the seismic input, it is essential to monitor local EDPs, in agreement with the requirement of code-based procedures which are conventionally used while using deterministic approaches.

Only few authors have investigated the seismic performances of existing structures by considering local EDPs. Amongst others, Freddi *et al.* [13] performed Incremental Dynamic Analyses (IDA) [18] to evaluate the fragilities for both the system and the components of a reinforced concrete frame retrofitted with buckling restrained braces. The outcomes show how the use of global EDPs may be inadequate in some situations. Similarly, Freddi *et al.* [14] investigated the definition of Probabilistic Seismic Demand Models for local EDPs while performing Cloud Analyses on a reinforced concrete frame. Song et al. [19] performed a probabilistic assessment of the seismic demands and fracture capacity of welded column splice connections, *i.e.*, local EDP, in steel MRFs. The study was based on Cloud and Montecarlo analyses and focused on two case study structures providing insights on the influence of relevant uncertainties on the assessment of fracture fragility of welded column splice connections.

The present paper compares the outcomes of assessment procedures performed by using capacity limits for component level EDPs (*i.e.*, local EDPs) established by European and American codes, in order to identify some challenges and to provide some preliminary insights for the revision of the Eurocode 8 Part 3. Two low-code MRFs, widely investigated in literature [*e.g.*, 20], were considered for case study purposes and the assessment was performed based on three local EDPs, *i.e.*, column's rotation, beam's rotation and panel zone's shear distortion, and the inter-story drift as global EDP. IDAs [18] are performed for the development of components and system fragility curves.

This paper is organised as follows: Section 2 provides a comparative review of the local EDPs related to steel MRFs and highlights the similarities and differences between the European and American assessment codes on this matter; Section 3 introduces two case study buildings, representative of low-code steel MRFs and provides details on the numerical models and on the outcomes of modal, non-linear and IDAs and provides a comparison between the system and components fragility curves considering the different investigated assessment codes. Finally, conclusions are made based on the observations in this paper, and comments are drawn on possible future paths for this research.

2 Code prescribed EDPs

The current study focuses on the comparison of assessment procedures performed by using capacity limits for component level EDPs (*i.e.*, local EDPs) based on different assessment codes. The considered codes are (1) the EC8-3 [3], which is the latest version of the European regulation for the assessment of existing structures; (2) the ASCE Standard 41-06 [8], which was strongly based in the ASCE Standard 31-03 [21] and FEMA 310 [22]; (3) the ASCE 41-13 [7], which is a revised version of its predecessor; and (4) the ASCE 41-17 [6], which establishes significant changes with respect to its predecessors and the European regulation.

2.1 Damage states

All of these codes establish discrete limits to characterise the boundaries between damage ranges. The European code defines three limit states, which describe both the structural and the non-

structural damage on the building. On the other hand, the American codes untie the structural and non-structural damage and define three structural performance levels and five non-structural performance levels. Even though the codes also describe the structures in terms of non-structural damage, this paper is solely focused on the structural damage in the building. The structural damage states are associated with capacity values (or acceptance criteria, as defined in the American codes) that permit to indirectly link the deformation (or force) demands to a specific state of damage in the structure.

Although the three limit states in the EC8-3 [3] and the corresponding structural performance levels in the ASCE41 [6, 7, 8] are not exactly defined in the same way for all codes, in this study, they are considered equivalent, in order to reduce the number of variables involved in the problem and to facilitate the comparison of the outcomes. The three Damage States can be broadly classified as: (1) Damage State 1 (DS1), which is correlated to a structure with only slight damage, in which the structural elements retain the pre-earthquake strength and stiffness; (2) Damage State 2 (DS2), which is associated to a damaged structure that shows some permanent drift, but retains some residual strength and stiffness and is capable of withstanding some lateral loads (*e.g.* moderate aftershocks): and (3) Damage State 3 (DS3), which is correlated to a near collapse building, damaged beyond repair, with large permanent drift and little residual strength and stiffness. Table 1 shows the described damage states as defined in the codes. A detailed description of the damage states is reported in the codes [3, 6, 7, 8]. It is worth mentioning that the EC8-3 ties each limit state to the probability of occurrence of the events that, coupled with the seismic hazard for the site, provide the seismic intensity. Conversely, the American codes, recommend performance objectives linked to different structural performance levels, but allow the stakeholders to make the final decision based on multiple factors. Considerations regarding the seismic intensity are out of the scope of this paper and the reader can refer to [5] for further discussion on this topic.

Table 1 Assumed equivalency of damage states among different codes

Code	Damage State 1	Damage State 2	Damage State 3
EC8-3	Damage Limitation	Significant Damage	Near Collapse
ASCE-41	Immediate Occupancy	Life Safety	Collapse Prevention

2.2 Engineering Demand Parameters

This paper focuses on the comparison of the main EDPs for a low-code steel MRF building, therefore, the considered EDPs are: (1) chord rotation in columns, (2) chord rotation in beams, and (3) panel zone shear distortion.

2.2.1 Chord rotation in columns

The main difference between the rotation capacity in beams and columns is related to the influence of the axial loads acting on the columns. This is acknowledged in the American codes considered here, by including a dimensionless axial demand to capacity ratio ($\nu = P/P_{ye}$), which affects, depending on the code, the rotation at yielding (θ_y) and the capacity limits.

Equations for the definition of the chord rotation at yielding (θ_y) are provided in the considered American codes [6, 7, 8] while the EC8-3 [3] does not give any indication on how to calculate it, therefore, it is assumed that the following analytical Equation (1) should be used for both beams and columns:

$$\theta_y = \frac{M_{pe} L}{6EI} \tag{1}$$

where θ_y is the chord rotation at yielding, $M_{pe} = ZF_{ye}$ is the expected plastic moment capacity, L is the length of the span or storey height, E is the Young's modulus, I is the moment of inertia, Z is the plastic section modulus and F_{ye} is the expected yielding stress of the material. As it can be observed, this formula does not consider the influence of the axial loads in the rotation capacity of the column, however, the code limits its applicability to columns with $\nu < 0.3$, and requests all the other elements to be treated as force elements (*i.e.*, no ductility considered).

The ASCE41-06 [8] and -13 [7] go a step further in the definition of θ_y by including terms related to the influence of the axial load, as follows:

$$\theta_y = \frac{M_{pe} L}{6EI}\left(1 - \frac{P}{P_{ye}}\right) \tag{2}$$

Finally, the ASCE 41-17 [6] also considers the influence of axial loads but in a more advanced way, by proposing a series of semi-empirical equations for different levels of normalised axial load ν, based on the work done by Lignos *et al.* [23]. In addition, this code also considers the shear stiffness contribution to the overall stiffness of the column. The reader must refer to the ASCE 41-17 [6] for details on these equations. It is worth highlighting that this version of the code uses the gravity axial load P_G instead of the total axial load P (*i.e.*, gravity plus overturning), in an attempt to simplify the assessment process and to avoid having to calculate the yielding rotation at each step of the time history (according to the commentary in [6]).

With respect to the plastic rotation capacity, each code defines limits depending on the slenderness of the flange, web and column itself. The EC8-3 [3] considers the slenderness based on the classification established in the Eurocode 3 Part 1-1 [24]. Only sections classified as 'Class 1' or 'Class 2' are capable of developing plastic rotation without local buckling, therefore, they are the only ones considered for the definition of plastic rotation damage states. Similarly, the American code requests the steel section to be seismically compact, as defined by AISC 341 [25], to allow the development of plastic deformations. Details on the slenderness limits should be observed directly in the respective code.

Table 2 summarises the rotation capacity values for columns for the different codes. A range of values is presented to summarise all the possible values that the code prescribes. In the EC8-3 [3], the values are directly assigned to Class 2 or Class 1 steel shapes, respectively. In the American codes [6, 7, 8], the values represent the minimum and maximum values prescribed by the code, however, the exact value depends on the slenderness of the web and flanges. As it can be observed, the values for the EC8-3 are similar to those in ASCE41-06 [8] for the elements with low axial loads. In contrast, subsequent editions of the American code allow larger rotation limits in the two highest damage states for the ASCE41-13 [7], but in all damage states for the ASCE41-17 [6], which also allows columns with relative axial demand of up to 0.6 and columns in tension.

The limits in the ASCE41-17 [6] are further relaxed by using P_G instead of P, as suggested in the code. Nonetheless, according to previous studies [*i.e.*, 23, 26, 27, 28] this simplification should not significantly affect the plastic rotation capacity of the column. The

Table 2 Plastic rotation capacity values for columns

Code	Relative axial demand	Damage State 1	Damage State 2	Damage State 3
EC8-3	$\nu \leq 0.3$	$0.25\,\theta_y$ or $1.0\,\theta_y$	$2.0\,\theta_y$ or $6.0\,\theta_y$	$3.0\,\theta_y$ or $8.0\,\theta_y$
ASCE-41-06	$\nu < 0.2$	$0.25\,\theta_y$ to $1.0\,\theta_y$	$2.0\,\theta_y$ to $6.0\,\theta_y$	$3.0\,\theta_y$ to $8.0\,\theta_y$
	$0.2 \leq \nu \leq 0.5$	$0.25\,\theta_y$	$0.5\,\theta_y$ to $8\left(1-\frac{5}{3}\frac{P}{P_{ye}}\right)\theta_y$	$0.8\,\theta_y$ to $11\left(1-\frac{5}{3}\frac{P}{P_{ye}}\right)\theta_y$
ASCE-41-13	$\nu < 0.2$	$0.25\,\theta_y$ to $1.0\,\theta_y$	$3.0\,\theta_y$ to $9.0\,\theta_y$	$4.0\,\theta_y$ to $11.0\,\theta_y$
	$0.2 \leq \nu \leq 0.5$	$0.25\,\theta_y$	$1.2\,\theta_y$ to $14\left(1-\frac{5}{3}\frac{P}{P_{ye}}\right)\theta_y$	$1.2\,\theta_y$ to $17\left(1-\frac{5}{3}\frac{P}{P_{ye}}\right)\theta_y$
ASCE-41-17	Refer directly to Table 9-7.1 in the code [6]			

Note: Specific capacity values depend on the slenderness of the analysed section. Refer to the code directly for slenderness limits.

aforementioned publications are based on the assumption of fixed maximum axial loads equivalent to 70 or 75% of the axial yielding capacity of the column, which is not necessarily the case in buildings with perimeter steel MRFs, particularly those with big floor areas or considerable height. The current version of the American code establishes that columns with $P_G/P_{ye} > 0.6$ must be treated as force elements, however, a column can yield due to overturning axial loads even if the gravity axial loads are relatively low, since the overturning loads depend mainly on the geometry of the frame, the distribution of masses and the intensity of the ground-motion. This could lead to cases in which columns that overpassed their axial capacity due to overturning forces, are treated as deformation-controlled elements, which is precisely the case in the buildings studied in this paper.

2.2.2 Chord rotation in beams

Beam rotations are established based on similar criteria to the rotation in columns, with the only exception that no axial loads are considered for these elements and therefore, the definition of θ_y is not affected by ν. Similar to the case of the columns, the EC8-3 does not establish an equation for θ_y, therefore, Equation (1) is usually considered. Both the ASCE41-06 [8] and -13 [7] request θ_y to be calculated by using Equation (1). Conversely, ASCE41-17 modifies this equation by adding a term to account for the shear stiffness of the section.

The slenderness limits for beams are established in as similar way to those in the columns, but vary considerably for the web since it is considered to work in bending rather than compression and therefore, it is less likely to develop local buckling. The capacity values are shown in Table 3. As it can be observed the values for the EC8-3 [3] and the ASCE41-06 [8] are similar. ASCE41-13 [7] increases the rotation capacity in the DS2 and DS3 while ASCE41-17 [6] keeps these increases but adds an increase also for the DS1. It is worth mentioning that the ASCE41-17 [6] allows much larger rotations for the DS1 with respect to the previous versions.

2.2.3 Panel zone shear distortion

The panel zone shear distortion limits are established to guarantee the ductility of the element before local buckling and to avoid large distortions that could cause a brittle failure in the surrounding welds. Although there are multiple force-based checks that should be performed on these structural elements, this paper is focused only on the capacity limits related to the deformations. The shear distortion is represented as a relative node rotation (*i.e.*, rotation between the column line and the beam line), therefore, it is also represented by θ_y, but in this case, this term refers to the rotation as consequence of the shear distortion at yielding. None of the codes provide equations to calculate θ_y, except the ASCE41-17 [6], which proposes the following Equation (3):

$$\theta_y = \frac{F_{ye}}{G\sqrt{3}}\sqrt{1-\left(\frac{|P_G|}{P_{ye}}\right)^2} \tag{3}$$

where G is the shear modulus.

As reported in Table 4, EC8-3 only establishes that the panel zones must remain elastic for the Damage Limitation limit state (*i.e.*, no plastic rotation). ASCE41-06 establishes limits for all structural performance levels, and ASCE41-13 makes them once again more permissive, as for other EDPs. It is worth noting that this code assigns the same numerical value to the DS2 and DS3. Similar values are used for ASCE41-17 when $\nu < 0.4$. However, when the gravity axial load overpasses this limit, the values are reduced.

Table 3 Plastic rotation capacity values for beams

Code	Damage State 1	Damage State 2	Damage State 3
EC8-3	$0.25\,\theta_y$ or $1.0\,\theta_y$	$2.0\,\theta_y$ or $6.0\,\theta_y$	$3.0\,\theta_y$ or $8.0\,\theta_y$
ASCE41-06	$0.25\,\theta_y$ to $1.0\,\theta_y$	$2.0\,\theta_y$ to $6.0\,\theta_y$	$3.0\,\theta_y$ to $8.0\,\theta_y$
ASCE41-13	$0.25\,\theta_y$ to $1.0\,\theta_y$	$3.0\,\theta_y$ to $9.0\,\theta_y$	$4.0\,\theta_y$ to $11.0\,\theta_y$
ASCE41-17	$1.0\,\theta_y$ to $2.25\,\theta_y$	$3.0\,\theta_y$ to $9.0\,\theta_y$	$4.0\,\theta_y$ to $11.0\,\theta_y$

Note: Specific capacity values depend on the slenderness of the analysed section. Refer to the code directly for slenderness limits.

Table 4 Plastic rotation capacity as consequence of shear distortion in panel zones

Code	Damage State 1	Damage State 2	Damage State 3
EC8-3	0	Not specified	Not specified
ASCE41-06	$1.0\,\theta_y$	$8.0\,\theta_y$	$11.0\,\theta_y$
ASCE41-13	$1.0\,\theta_y$	$12.0\,\theta_y$	$12.0\,\theta_y$
ASCE41-17*	$1.0\,\theta_y$ or $\frac{5}{3}\left(1-\frac{\lvert P_G\rvert}{P_{ye}}\right)\theta_y$	$12.0\,\theta_y$ or $20\left(1-\frac{\lvert P_G\rvert}{P_{ye}}\right)\theta_y$	$12.0\,\theta_y$ or $20\left(1-\frac{\lvert P_G\rvert}{P_{ye}}\right)\theta_y$

*The values used in ASCE41-17 depend on the relative axial load, with the first value used for $|P_G| < 0.4$, and the second value used otherwise.

3 Case studies Assessment

Two steel MRFs which were originally designed with code provisions that nowadays are considered outdated, either due to the reclassification of seismic hazard maps, or due to the update of the design codes are considered as case study structures. These structures were selected among those designed for the SAC project, coordinated by the Federal Emergency Management Agency (FEMA) and detailed in Gupta and Krawinkler [20]. The comparison of the assessment procedures of the different capacity limits and of the different components relies on IDAs [18] that allow the definition of system and components level fragility curves.

3.1 Characteristics of the structures

The two case study buildings were designed as located in Boston (*i.e.*, low seismicity), built on stiff soil, designed for office occupancy, with regular plan distribution and with no considerable irregularities along the height. These buildings were intended to be representative of low- and mid-rise steel MRFs, (*i.e.*, 3 and 9 storeys). For the sake of brevity, the buildings will hereafter be referred as 3B and 9B, respectively. Both structures were designed according to the 12th edition of the National Building Code (as noted by [20]), considering gravity, seismic and wind loads. Since the seismic demand for the site is very low, the seismic forces only controlled the design of 3B, while 9B design was controlled by wind loads [20]. In both cases, the lateral loads were resisted by perimeter steel MRFs, while the majority of the gravity loads were resisted by internal gravity frames, as it was common practice for this kind of structures in the early 90's in the USA. Similarly to [20], this paper only considers the frames oriented on the N-S direction and neglects the torsional effects. Therefore, only the planar structure is analysed with its corresponding tributary mass (*i.e.*, half of the building's mass). The elevation views for buildings 3B and 9B are shown in Figure 1. The seismic mass for both buildings is reported in Table 5.

In addition to the different number of storeys, both buildings differ in the plan distribution and lateral frame global geometry. In fact, in the 9B, the designers decided to add an extra span with a beam simply supported on a corner column, which is oriented on its weak axis. Additional details on the design criteria for the buildings can be found in [20].

3.2 Finite element models

Two-dimensional non-linear finite element (FE) models of the frames were developed in the Open System for Earthquake Engineering Simulation (OpenSees) [29]. Columns were modelled based on the distributed plasticity approach to account for the interaction of axial and bending stresses, while beams were modelled based on the lumped plasticity approach (*i.e.*, non-linear rotational springs plus elastic beam elements). The plastic hinges on the beams were calibrated based on the model proposed by Lignos and Krawinkler [30], modified under the approach suggested by Zareian and Medina [31], in order to compensate the flexibility and the damping properties of the beams. In addition, panel zones were modelled according to the 'Scissors model' [32]. The material properties are defined according to the design, *i.e.*, ASTM A572 Grade 50 (Group 1) steel in all beams and columns (F_y = 344.74 MPa; E = 199.95 GPa). The nominal value of F_y was further increased by 10% to account for the material overstrength, according to ASCE41-17 [6].

Damping was considered by using mass- and stiffness proportional damping (Rayleigh Damping), with a damping ratio $\zeta = 3\%$. The contribution of geometric second order effects (P-Δ) of the gravity frame was considered by including a parallel leaning column, which concentrates the area and moment of inertia of the gravity columns, and is connected by rigid links at each storey to the rest of the structure. This column was modelled as pinned element at the base to neglect its contribution to the lateral resisting system, however, the bending stiffness along the height of the column was kept to provide the structures with a spine-like element that contributes towards the uniformity of the deformed shape along the buildings' height. This is especially critical in buildings with weak main lateral resisting systems since neglecting this contribution may derive in unrealistic soft-storey mechanisms.

3.3 Modal and non-linear static analyses

The first and second periods of vibration are respectively T_1= 1.85 sec and T_2 = 0.51 sec for the building 3B and T_1= 3.27 sec and T_2 = 1.21 sec for the building 9B. These periods are in agreement with previous studies that were analysing the same case study structures, *i.e.*, Gupta and Krawinkler [20].

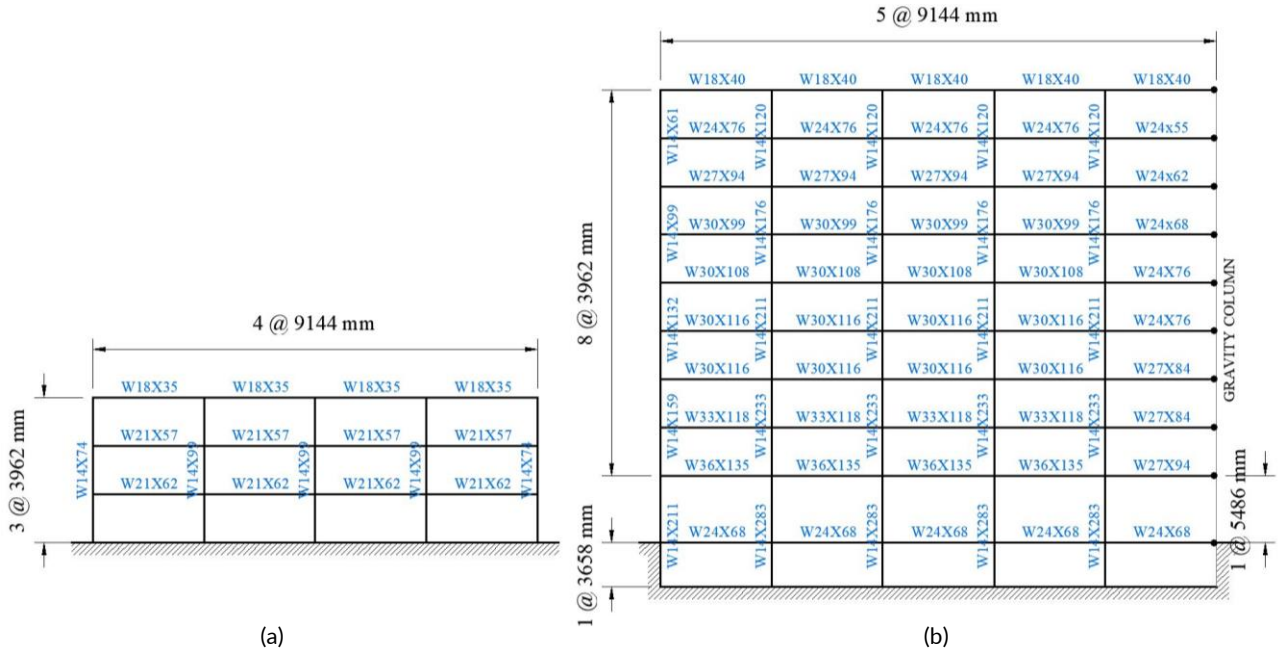

Figure 1 Dimensions of N-S perimeter steel MRF for (a) building 3B and (b) building 9B, as reported in [20]

Non-linear static analyses, with lateral loads proportional to their first mode of vibration and storey mass distribution, were performed on both structures and the results are shown in Figure 2. The IDR in the building 3B was found to be similar among its storeys at different stages of the pushover analysis. On the other hand, the building 9B shows a different behaviour among its storeys, particularly at the 1st storey, which, due to the higher inter-storey height, is softer when compared to its adjacent storeys. It is important to highlight that the behaviour of the structure is heavily influenced by the uniformity contribution of the leaning column, therefore, deformation at each storey is mainly controlled by rotation in the panel zones, which is consistent with the analysis made in [20] for these case study structures.

Table 5 Seismic masses per storey for building 3B and 9B

Building 3B		Building 9B	
Storey	**Mass (ton)**	**Storey**	**Mass (ton)**
1	956.64	**1**	1009.19
2	956.64	**2 to 8**	991.73
3	1035.41	**9**	1069.29

3.4 Ground motion input

A set of 22 recorded far-field Ground Motion (GMs) developed by the ATC-63 project [33] were used for the non-linear time history analyses and to perform IDAs [18]. The GMs were recorded on stiff soil, do not exhibit pulse-type characteristics (*i.e.*, source-to-site distance higher than 10 km).

The spectral acceleration corresponding to the first structural period $S_a(T_1)$ calculated with an inherent damping ratio of 3% is used as Intensity Measure (IM). This structure-dependent IM has been demonstrated by many authors to provide a 'good' correlation with structure's EDPs and hence with the damage (*e.g.* [14]). However, this IM neglects the spectral shape of the GMs that could significantly influence the response under higher modes especially in tall buildings [34]. Other advanced IMs, such as vector value IMs [35] or the average S_a [36] could be considered for future development of the work in addressing this drawback.

Figure 3 shows the scaled GM spectra used for the IDA, with an IM such that the $S_a(T_1)$ value is equal to g. It can be observed that, the dispersion of S_a values used for higher modes is greater for the building 9B, due to the impact of the scaling at lower regions of the spectrum (*i.e.*, the scaling factors have a higher impact when the reference S_a is smaller).

3.5 Incremental Dynamic Analysis (IDA)

The aforementioned GMs were scaled to different values of IM to cover the whole range from elastic to non-linear seismic response to perform IDAs. For building 3B, the scaling went from 0.01g to 0.35g, while building 9B was subjected to GMs scaled to IM values from 0.01g to 0.20g. All of the local EDPs related to this study were recorded, as well as the IDR as global EDP, in order to be able to understand how the local EDPs relate to global demands on these structures. Due to the regularity of the buildings, many local EDPs deform consistently along each floor, however, it was considered that a damage state is surpassed when the first element of each type exceeds the capacity limits, as indicated by the codes [3, 6, 7, 8]. The redistribution of forces and the definition of the failures at storey level is beyond the scope of this paper, but the interested reader is referred to Pinto and Franchin [37] for further discussion.

Figure 4 shows the comparison of the considered EDPs for both buildings. In particular, in this figure, the local parameters are reported as normalized with respect to their yielding capacity values. As it can be observed, both buildings exhibit a non-linear behaviour mainly controlled by the yielding in the panel zones.

The weakness in the panel zones is consistent with pre-Northridge buildings conceived without capacity design considerations. An aspect to highlight is the higher dispersion on the EDPs related to building 9B. This can be attributed to the higher number of components considered, the impact of higher modes on the structural behaviour, and the higher variability of the IM for periods different than T_1.

3.6 Fragility analysis

In order to compare the assessment procedures performed by using capacity limits for component level EDPs (*i.e.*, local EDPs) based on different assessment codes, fragility curves are derived for the systems and for the components.

The fragility curves are shown in Figure 5. Each graph shows a comparison of the fragility curves for all damage states and for all the considered EDPs, according to the different codes and for both buildings 3B and 9B. In addition, a reference set of fragility curves based on the IDR limits established by ASCE41-06 [8] is included in

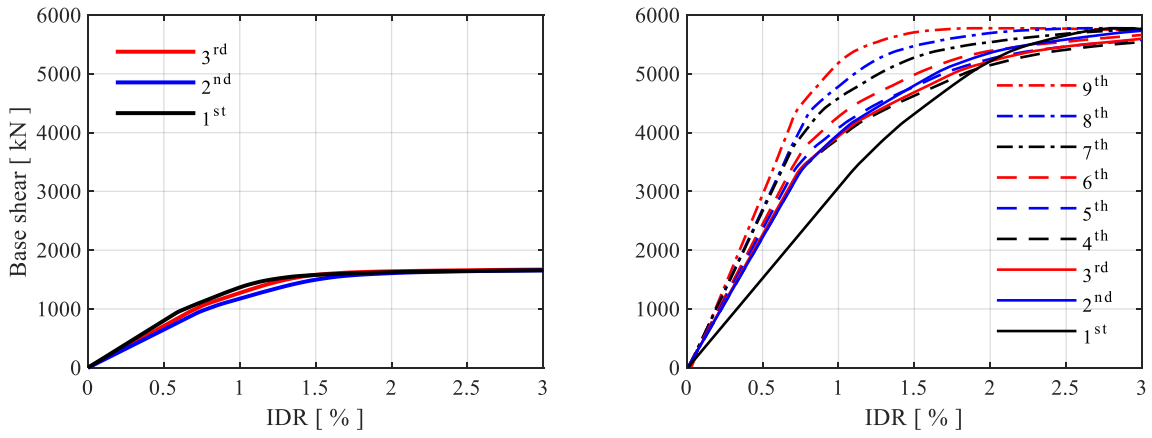

Figure 2 Pushover curves for (a) building 3B and (b) building 9B

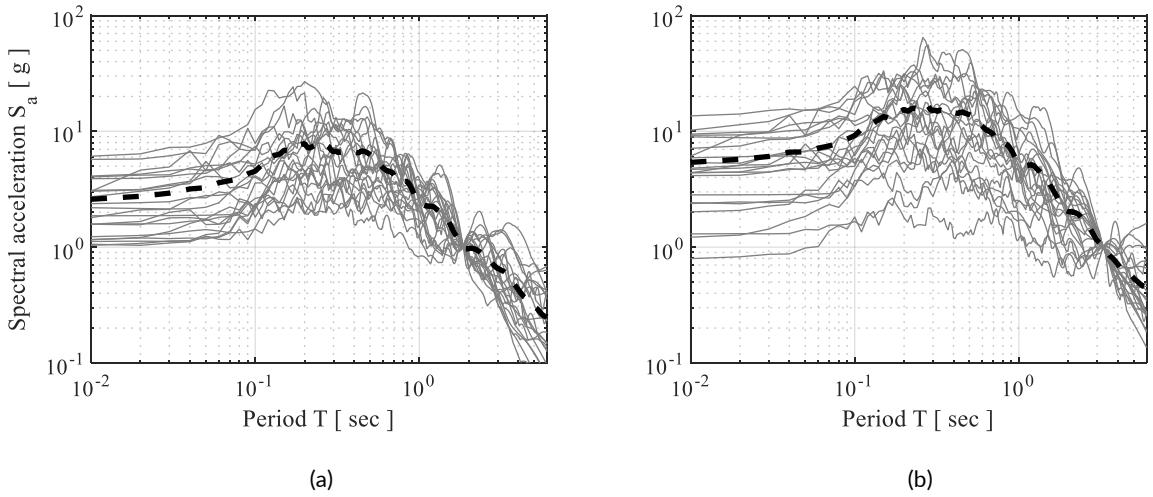

Figure 3 Pushover curves for (a) building 3B and (b) building 9B

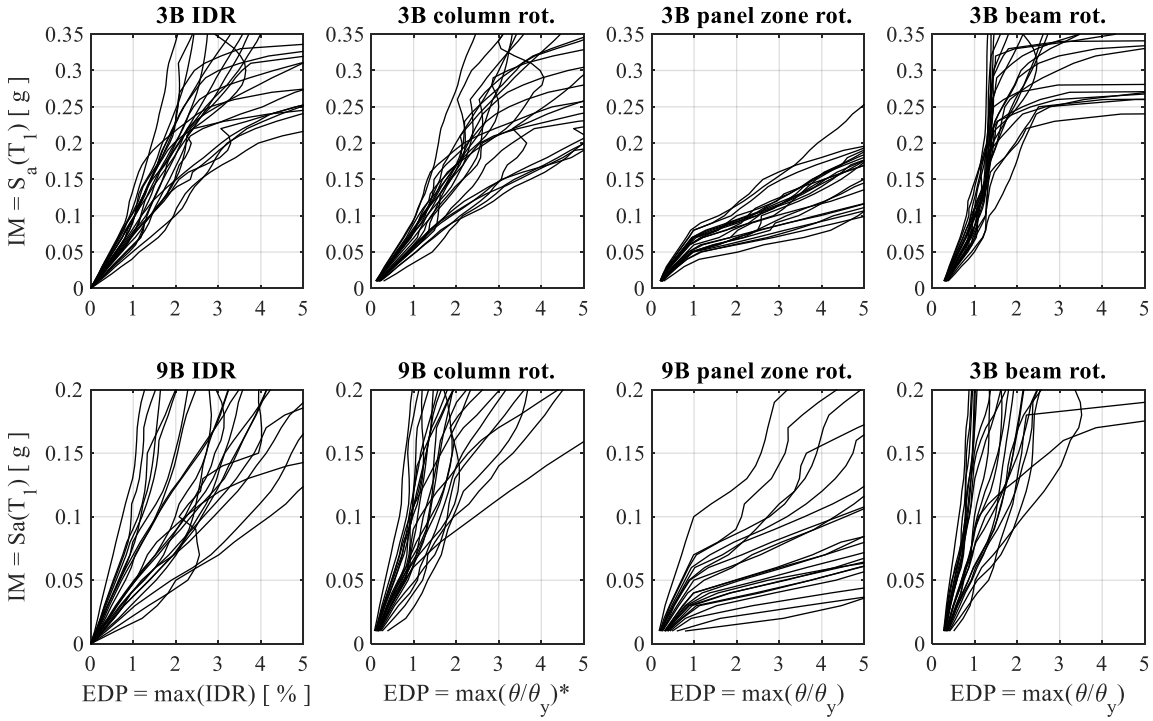

Figure 4 Comparison of different EDPs related to the most critical element on each building. *Yield rotation in columns was defined considering also the axial load, as indicated in ASCE41-06/13

all the figures to facilitate the comparison between the fragilities obtained by the different codes. These fragility curves are representative of IDRs of 0.7%, 2.5% and 5.0%, for the DS1, DS2 and DS3, respectively.

The DS1 is represented by green curves for all EDPs. Similarly, yellow curves represent the fragility curves related to DS2, and red curves are related to DS3. Each type of EDP is represented with a different type and thickness of line, to facilitate the comparison among EDPs. The fragility curves corresponding to the reference IDR limits are coloured in different shades of grey.

For DS1, it is observed that the panel zones are the most fragile components in all cases. As expected, panel zones' fragility for EC8-3 [3] has more conservative values, as the deformations are limited to the elastic range. The rest of the considered codes show the same fragility curve as they are all based on the same capacity value.

However, for DS2 and DS3, the controlling EDP changes from code to code. For example, in EC8-3 [3], due to the lack of capacity limits for the panel zones, the governing EDP is the plastic rotation of columns. It would be necessary to perform additional checks in the panel zones to guarantee their integrity at such level of distortion. For the ASCE41-06 [8] and -13 [7], the fragility curves corresponding to panel zone distortion and column rotation show very similar values in building 3B, however, building 9B is governed by the distortion in panel zones. Finally, ASCE41-17 [6] show that the fragility is directed by the distortion in panel zones in all cases. This observation becomes more accentuated in building 9B, in comparison to building 3B, due to the higher relative bending stiffness that columns and beams have with respect to the panel zones.

With the only exception of the EC-8 [3] for the building 9B, the fragility curves for beams show the lowest probability of exceedance of all EDPs.

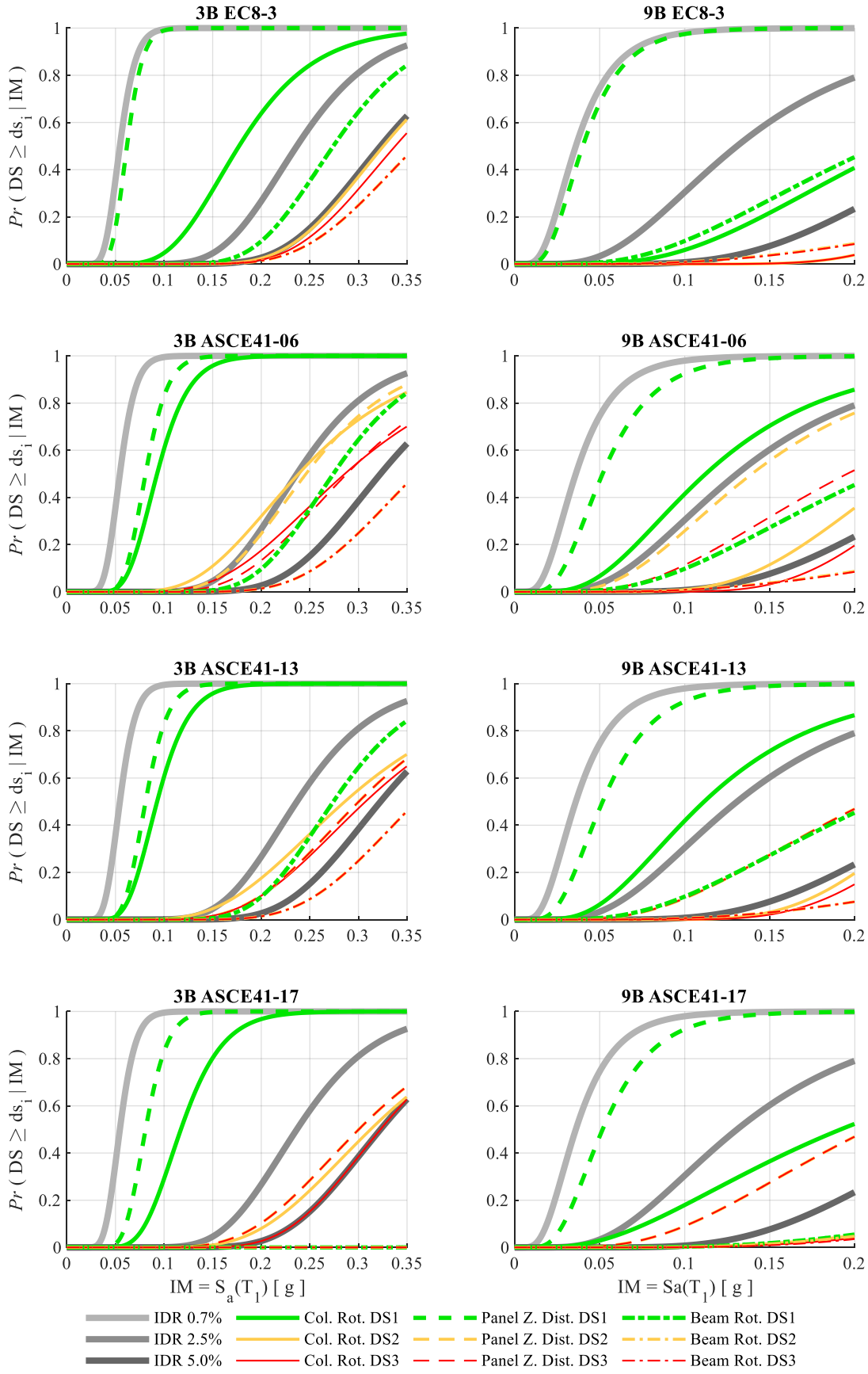

Figure 5 Comparison of fragility curves for different EDPs for buildings 3B and 9B, based on the different considered codes

Conclusions

The probabilistic assessment of the seismic performance of steel Moment Resisting Frames (MRFs), including the effect of the record-to-record variability, is commonly made by using global Engineering Demand Parameters (EDPs), such as the inter-storey drift ratio (IDR).

However, global EDPs may not be adequate to synthetically represent the seismic performance of structures that were designed without modern seismic design provisions (*e.g.*, capacity design). In fact, due to the lack of seismic design rules, there may be no relationship between local failures and global EDPs. In these cases, local EDPs should be used, in agreement with the requirement of code-based procedures which are conventionally used while using deterministic approaches.

This paper investigates and compares the assessment procedures by using code established capacity limits for component level EDPs such as rotations in columns, rotations in beams and shear distortions in panel zones. Four modern assessment codes were considered: EC8-3, ASCE41-06, ASCE41-13 and ASCE41-17.

The study identified some of the main drawbacks of the EC8-3 with respect to the latest version of the American standard. Amongst other omissions, there are no capacity limits for panel zones' distortion at Significant Damage and Near Collapse limit states, or clear formulations to determine the yielding capacity of the local elements. Additionally, there is a lack of considerations regarding the simultaneous effects of actions, such as axial and shear loads.

In order to assess the impact of the studied EDPs in a low-code steel MRF, two case study buildings were analysed in an Incremental Dynamic Analysis framework, to develop fragility curves at each damage state and for each local EDP. It was found that the case study buildings' fragility is mainly controlled by the shear distortion in the panel zones, which is consistent with the design deficiencies of pre-Northridge buildings. This observation is even more significant in building 9B than in building 3B, due to the higher relative bending stiffness that columns and beams have with respect to the panel zones.

In comparison, the considered American codes have evolved towards a less conservative direction by increasing the capacity limits for all EDPs in the newer versions, which is reflected in the fragility curves. For the case of building 3B, the impact of neglecting the overturning axial forces in ASCE41-17 is not enough to significantly differentiate from its predecessors. However, that is not the case in building 9B, in which there is a significant change with respect to ASCE41-13 and -06. Fragility of buildings assessed under the limits established by EC8-3 show more conservative values than when assessed by the American codes, except when the rotation in columns is used as EDP. For this particular EDP, the fragility curves are similar to those in the ASCE41-17 in both case study buildings.

One of the limitations of this study is that it does not account for other failure modes such as rupture and buckling in the panel zones, or rupture of the surrounding welds. Future stages of this work might consider these effects, as well as building collapse. In addition, other building typologies and design levels may be assessed in order to understand better the impact of using local EDPs at each of those building configurations.

The outcomes of this study provides useful insights for the development of the next generation of the European assessment code.

Acknowledgements

This research was partially funded by CONACYT-FiiDEM (Grant No. 2018-000013-01EXTF-00148). Any opinions, findings, and conclusions or recommendations expressed in this paper are those of the authors and do not necessarily reflect the views of the funding agencies.

References

[1] Federal Emergency Management Agency (2000) State of the Art Report on Systems Performance of Steel Moment Frames Subject to Earthquake Ground Shaking. *FEMA-355C*. Washington, USA.

[2] Jaiswal, K., Waldederal, D.J. (2008) Creating a Global Building Inventory for Earthquake Loss Assessment and Risk Management. *U.S. Geological Survey Open-File Report 2008-1160*. Reston, USA.

[3] European Committee for Standardization (2005) Eurocode 8: Design of structures for earthquake resistance – Part 3: Assessment and retrofitting of buildings. *EN 1998-3*.

[4] Araújo, M., Castro, J.M. (2016) On the quantification of local deformation demands and adequacy of linear analysis procedures for the seismic assessment of existing steel buildings to EC8-3. *Bulletin of Earthquake Engineering* **14**, 1613-1642.

[5] Araújo, M., Castro, J.M. (2018) A critical review of European and American provisions for the seismic assessment of existing steel moment-resisting frame buildings. *Journal of Earthquake Engineering* **22**(8), 1336-1364.

[6] American Society of Civil Engineers, Structural Engineering Institute (2017) Seismic Evaluation and Retrofit of Existing Buildings. *ASCE/SEI 41-17*. Reston, USA.

[7] American Society of Civil Engineers, Structural Engineering Institute (2013) Seismic Evaluation and Retrofit of Existing Buildings. *ASCE/SEI 41-13*. Reston, USA.

[8] American Society of Civil Engineers, Structural Engineering Institute (2007) Seismic Rehabilitation of Existing Buildings. *ASCE/SEI 41-06*. Reston, USA.

[9] Araújo, M., Macedo, L., Castro, J.M. (2017) Evaluation of the rotation capacity limits of steel members defined in EC8-3. *Journal of Constructional Steel Research* **135**, 11-29.

[10] Kwon, O.S., Elnashai, A. (2006) The effect of material and ground motion uncertainly on the seismic vulnerability curves of RC structure. *Engineering Structures* **28**(2), 289-303.

[11] Tubaldi, E., Barbato, M., Dall'Asta, A. (2012) Influence of model parameter uncertainty on seismic transverse response and vulnerability of steel-concrete composite bridges with dual load path. *Journal of Structural Engineering* **138**(3), 363-374.

[12] Hueste, M.D., Bai, J.W. (2006) Seismic Retrofit of a Reinforced Concrete Flat-Slab Structure: Part II – Seismic Fragility Analysis. *Engineering Structures* **29**(6), 1178-1188.

[13] Freddi, F., Tubaldi, E., Ragni, L., Dall'Asta, A. (2013) Probabilistic performance assessment of low-ductility reinforced concrete frames retrofitted with dissipative braces. *Earthquake Engineering & Structural Dynamics* **42**, 993-1011.

[14] Freddi, F., Padgett, J.E., Dall'Asta, A. (2017) Probabilistic seismic demand modeling of local level response parameters of an RC frame. *Bulletin of Earthquake Engineering* **15**(1), 1-23.

[15] Molina Hutt, C., Rossetto, T., Deierlein, G. (2019) Comparative risk-based seismic assessment of 1970s vs modern tall steel moment frames. *Journal of Constructural Steel Research* **159**, 598-610.

[16] Baker, J.W., Cornell, C.A. (2006) Spectral shape, epsilon and record selection, *Earthquake Engineering & Structural Dynamics* **35**, 1077–1095.

[17] Zareian, F., Krawinkler, H. (2007) Assessment of probability of collapse and design for collapse safety. *Earthquake Engineering & Structural Dynamics*. **36**, 1901-1914.

[18] Vamvatsikos, D., Cornell, C.A. (2002) Incremental dynamic analysis. *Earthquake Engineering & Structural Dynamics* **31**(3), 491-514.

[19] Song, B., Galasso, C., Kanvinde, A. (2020) Advancing fracture fragility assessment of pre-Northridge welded column splices. *Earthquake Engineering and Structural Dynamics*, **49**, 132-154.

[20] Gupta, A., Krawinkler, H. (1999) Seismic demands for performance evaluation of steel moment resisting frame structures. *Report 132 SAC Task 5.4.3*. Stanford University, Stanford, USA.

[21] American Society of Civil Engineers, Structural Engineering Institute (2003) Seismic Rehabilitation of Existing Buildings. *ASCE/SEI 31-03*. Reston, USA.

[22] Federal Emergency Management Agency (1998) Handbook for the Seismic Evaluation of Buildings – A Prestandard. *FEMA-310*, California, USA.

[23] Lignos, D. G., Hartloper, A. R., Elkady, A., Deierlein, G. G., Hamburger, R. (2019) Proposed updates to the ASCE 41 nonlinear modeling parameters for wide-flange steel columns in support of performance-based seismic engineering. *Journal of Structural Engineering* ***145***(9), 04019083.

[24] European Committee for Standardization (2005) Eurocode 3: Design of Steel Structures – Part 1-1: General Rules and Rules for Buildings. *EN 1993-1-1*.

[25] American Institute of Steel Construction (2016) Seismic Provisions for Structural Steel Buildings. *AISC 341-16*. Chicago, USA.

[26] Elkady, A., Lignos, D. G. (2015) Effect of gravity framing on the overstrength and collapse capacity of steel frame buildings with perimeter special moment frames. *Earthquake Engineering & Structural Dynamics* ***44***(8), 1289-1307.

[27] Suzuki, Y., Lignos, D. G. (2015) Large scale collapse experiments of wide flange steel beam-columns. *8th International Conference on Behavior of Steel Structures in Seismic Areas (STESSA)*.

[28] Cravero, J., Elkady, A., Lignos, D. G. (2020) Experimental evaluation and numerical modeling of wide-flange steel columns subjected to constant and variable axial load coupled with lateral drift demands. *Journal of Structural Engineering* ***146***(3), 04019222.

[29] McKenna, F., Fenves, G.L., Scott, M.H. (2000) Open system for earthquake engineering simulation. University of California, Berkeley, USA.

[30] Lignos, D.G., Krawinkler, H. (2011) Deterioration modeling of steel components in support of collapse prediction of steel moment frames under earthquake loading. *Journal of Structural Engineering* **137**, 1291-1302.

[31] Zareian, F., Medina, R.A. (2010) A practical method for proper modeling of structural damping in inelastic plane structural systems. *Computers and Structures* **88**, 45-53.

[32] Charney, F., Downs, W. (2004) Modelling procedures for panel zone deformations in moment resistin frames. *Connections in Steel Structures V. ESSC/AISC Workshop*, Amsterdam, Netherlands.

[33] Applied Technology Council (2008) Quantification of building seismic performance factors. *FEMA P-695 ATC-63 Project*. California, USA.

[34] Silva, V., Akkar, S., Baker, J.W., Bazzurro, P., Castro, J.M., Crowley, H., Dolsek, M., Galasso, C., Lagomarsino, S., Monteiro, R., Perrone, D., Pitilakis, K., Vamvatsikos, D. (2019) Current challenges and future trends in analytical fragility and vulnerability modeling. *Earthquake Spectra* **35**(4), 1927-1952.

[35] Baker, J.W., Cornell, C.A. (2007) Vector-valued intensity measures incorporating spectral shape for prediction of structural response. *Journal of Earthquake Engineering* **12**(4), 534-554.

[36] Kohrangi, M., Kotha, S.R., Bazzurro, P. (2017) Ground-motion models for average spectral acceleration in a period range: direct and indirect methods. *Bulletin of Earthquake Engineering* **16**(1), 45-65.

[37] Pinto, P.E., Franchin, P. (2008) Assessing existing buildings with Eurocode 8 Part 3: a discussion with some proposals. *Background documents for the "Eurocodes background and applications" workshop*. Brussels, Belgium.